Digital Coherent Receivers for Long-Reach Optical Access Networks

Domaniç Lavery, *Student Member, IEEE*, Robert Maher, *Member, IEEE*, David S. Millar, *Member, IEEE*, Benn C. Thomsen, *Member, IEEE*, Polina Bayvel, *Fellow, IEEE*, and Seb J. Savory, *Senior Member, IEEE*

***Abstract*—The relative merits of coherent-enabled optical access network architectures are explored, with a focus on achievable capacity, reach and split ratio. We review the progress in implementing the particular case of the ultra dense wavelength division multiplexed (UDWDM) passive optical network (PON), and discuss some challenges and solutions encountered. The applicability of digital signal processing (DSP) to coherent receivers in PONs is shown through the design and implementation of parallelized, low-complexity application-specific digital filters. In this work, we focus on mitigating the impact of local oscillator laser (LO) relative intensity noise (RIN) on receiver sensitivity, and propose an algorithm which compensates for this impairment. This phenomenon is investigated theoretically and then experimentally by evaluating the sensitivity of a coherent receiver incorporating different tunable light sources; a low-RIN external cavity laser (ECL) and a monolithically integrated digital supermode distributed Bragg reflector (DS-DBR) laser. It is shown that the RIN of the signal laser does not significantly contribute to the degradation of the receiver sensitivity. Finally, a 10 Gbit/s coherent PON is demonstrated using a DS-DBR laser as the LO laser. It is found that a receiver sensitivity of -38.8 dBm is achievable assuming the use of hard-decision forward error correction.**

***Index Terms*—Optical access, ultra dense (UD), wavelength division multiplexing (WDM), passive optical network (PON), digital signal processing (DSP).**

I. Introduction

COHERENT receivers were originally of interest in optical communications due to the high receiver sensitivities which they can achieve. They have since been combined with advanced digital postprocessing to enable the long transmission distances and high spectral efficiencies required for core networks. Coherent receivers are now being researched for use in access networks, although here it is the frequency selectivity of coherent receivers which has been of particular interest.

Investigations into coherent access have come as a result of exponential growth in bandwidth demands for both the wired and wireless domains. Telecommunications providers are faced with the dual challenge of reducing operating costs while increasing the bandwidth available to end users. Though there have been several proposals for optical access networks which achieve this, the most promising approach is the long-reach passive optical network (LR-PON). Here, a long (60–100 km) feeder fiber is used to extend the reach of the access network allowing a large number of optical network units (ONU) to be supported by a single optical line terminal (OLT). The additional advantage of this approach is that the metro area network can be completely replaced by a single, passive, fiber backhaul, leading to many reductions in expenditure, notably from real estate [1].

A key requirement for network consolidation is a high split ratio which takes advantage of this extended reach, and it is the method of this split, as well as the transceiver technology, that differentiates LR-PON designs. However, there is a consensus that wavelength division multiplexing (WDM) will be used to take advantage of the large optical fiber bandwidth.

In this work, we provide an overview of research in this area; highlighting the relative merits of several coherent detection schemes. In Section II, LR-PON architectures are detailed which each employ coherent detection to some degree. These are compared to a more conventional PON employing direct-detection receivers. Section III describes the design and design challenges of a network architecture which employs phase- and polarization-diverse coherent receivers in both the OLT and the ONU. This architecture relies on the use of a tunable local oscillator (LO) laser, and so we provide some performance metrics for the tunable semiconductor lasers used in this work. The remainder of the paper details a feasibility study of this network architecture, focussing on the use of tunable semiconductor lasers. Section IV outlines the experimental configuration used for this investigation, while Section V details our implementation of digital signal processing (DSP) algorithms, including a novel method for compensating relative intensity noise (RIN). The results of this investigation are given in Section VI with conclusions in Section VII.

II. Long-Reach PON Designs

Extending the reach of optical access networks beyond the 20 km specified by the gigabit-capable PON (GPON) standard has the potential to significantly cut operational costs through network consolidation. However, this is not a new idea. The amended GPON standard permits the use of a reach extender to enable standards-compliant transmission over 60 km while doubling the split ratio to 1:64 [2] (or even 1:128 as permitted by the original standard [3]). An example of an extended-reach GPON

Manuscript received June 29, 2012; revised August 30, 2012, September 28, 2012; accepted September 28, 2012. Date of publication October 15, 2012; date of current version January 14, 2013. This work was supported in part by Oclaro Inc., in part by the EPSRC and in part by the European Commission PIANO+ project, CRITICAL.

D. Lavery, R. Maher, B. C. Thomsen, P. Bayvel, and S. J. Savory are with the Optical Networks Group, UCL Electronic and Electrical Engineering, Torrington Place, London, WC1E 7JE, U.K. (e-mail: d.lavery@ee.ucl.ac.uk).

D. S. Millar was with the Optical Networks Group, UCL Electronic and Electrical Engineering, Torrington Place, London, WC1E 7JE, U.K. He is now with Mitsubishi Electric Research Laboratories, Cambridge, MA 02139 USA (e-mail: millar@merl.com).

Color versions of one or more of these figures in this paper are available online at http://www.ieeexplore.ieee.org.

Digital Object Identifier 10.1109/JLT.2012.2224847

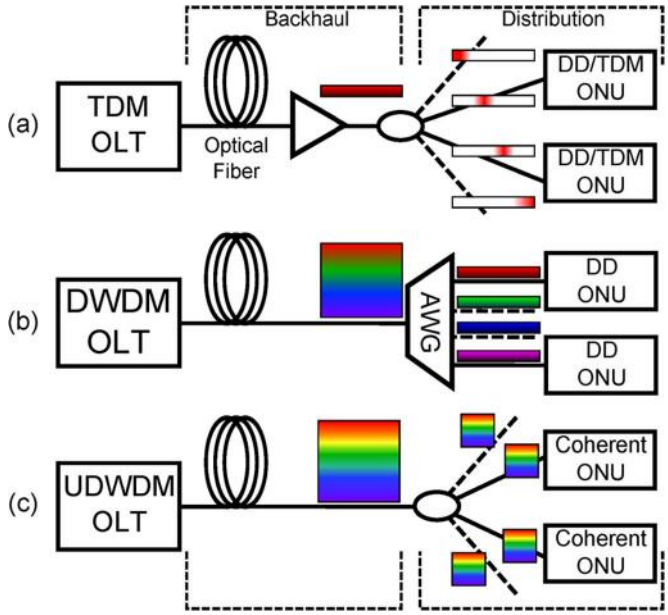

Fig. 1. Long-reach PON architectures. The backhaul section is typically 80–90 km with a passive distribution section of 10–20 km. (a) TDM-PON (for a GPON, the entire fiber length is limited to 60 km), (b) WDM-PON, (c) coherent UDWDM-PON.

employing a midspan erbium-doped fiber amplifier (EDFA) is shown in Fig. 1(a). The difficulty with this approach is that the aggregate capacity of the network (2.4 Gbit/s symmetric) does not change as, ultimately, all the ONUs are served by a single wavelength pair modulated using time-division multiplexing (TDM).

One approach to remove the requirement of midspan amplification is to split the signal after the fiber backhaul by using an arrayed waveguide grating (AWG), as in [4]; avoiding penalties due to passive splitting while effectively dedicating a wavelength to each ONU, as shown in Fig. 1(b). The disadvantage of this approach is that it colors the network, reducing the options for reconfigurability and presenting a challenge for inventory and deployment. For example, each transmitter needs to operate on a wavelength which is locked to the passband of the AWG, while the upstream channel from an ONU must be matched to its particular port on the AWG. This problem can be overcome to some extent through the transmission of a seed comb from the OLT which is remodulated (usually using a reflective semiconductor optical amplifier) at the ONU for upstream transmission, thereby avoiding the need for *a priori* knowledge of the network configuration. (Having a colorless ONU neatly solves inventory issues, because every ONU is identical.) However, the additional noise added to the carrier through amplification and remodulation dramatically reduces the power budget of the upstream signal. Conveniently, because the seed wavelength is generated at the OLT, homodyne coherent detection is used in this case to overcome these additional losses [5]. This also means that an advanced modulation format (such as QPSK) can be used for upstream transmission, reducing the electrical bandwidth requirements of the transmitter [5].

The reach and capacity limits of direct detection (DD) receivers for optical access have recently been explored without resorting to remodulation techniques. The hybrid WDM-TDM network is effectively a combination of the architectures shown in Fig. 1(a) and (b). Here, the ONU is made colorless by incorporating a piezo-electrically controlled tunable laser for upstream transmission. Recent work demonstrated impressive reach (100 km) and split ratios of 1:512 per wavelength when using 32-channel WDM; effectively supporting up to 16384 ONUs on a single PON [6], [7]. Due to the low sensitivity of direct detection receivers, the signal required multiple regenerations using EDFAs at a local exchange meaning that only the distribution section of the network was truly passive. With this configuration, not all of the economic benefits of long reach can be realized because the local exchange is still required to house equipment. Additionally, because the network is still based on TDM, the data rate per user is limited to 20 Mbit/s.

It was recently suggested that fully coherent networks would be an economically feasible way to increase network capacity, even if this involved coherent receivers at the ONU (for example, [8]–[10]).

The proposed architecture, Fig. 1(c), involves transmission of an ultra-dense WDM (UDWDM) source from the OLT and a passive midspan split such that each wavelength is simultaneously sent to every ONU. The channel of interest is then selected by retuning the LO laser in the ONU to generate a frequency offset between the channel of interest and the LO (Table I); this heterodyne receiver provides coherent gain that rejects the adjacent channels while avoiding the use of narrow-band tunable optical filters. The upstream channels are generated by splitting the LO for use as the signal, and frequency converting the signal before modulation and transmission. Provided the LO has tuned to the downstream channel, the upstream comb is automatically fixed to a grid.

This network architecture is completely reconfigurable because all downstream channels are sent to all receivers. For example, if a user wished to increase available bandwidth, additional ONUs could be situated at the access point. Each ONU adds an additional wavelength for communication, effectively scaling capacity at that location. However, the disadvantage of using a colorless splitter is the division of optical power between ONUs. If the power budget is too low to support this, an AWG could be used instead (as in the above scenario), but at the expense of dynamic reconfigurability. A hybrid solution is to use a coarse WDM demultiplexer (an AWG with a high free spectral range) followed by passive splitters. In this way, the network can be partially reconfigured while reducing the required power budget.

A simple example of this approach is coherent on-off keying (OOK) [10]. Here, only a single photodiode is required to detect the OOK signal (as in the DD case) however, coherent gain from the LO permits a denser channel spacing than could be realistically achieved with optical filters (for example an AWG) while also being reconfigurable through retuning the LO. An additional advantage of this approach is that the receiver sensitivity can approach the theoretical limit without narrow-band optical filters[1].

[1]Note that noise from transimpedance amplifiers, finite LO power and LO noise sources all prevent such receivers attaining the theoretical sensitivity limit in practice.

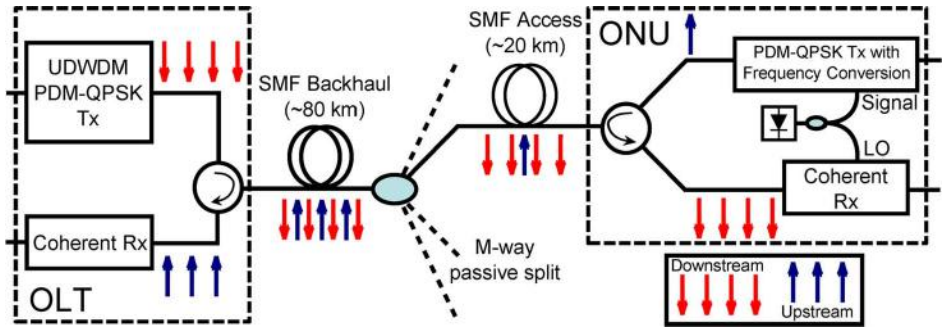

Fig. 2. Schematic of a coherent long-reach PON, with the frequency plan shown at key points. Note that the LO from the ONU can also be remodulated as the upstream channel, provided the LO channel is already set from the downstream comb.

TABLE I
REQUIRED COHERENT RECEIVER BANDWIDTHS

Coherent Receiver Type	Intradyne Frequency (IF)	Minimum Bandwidth
Homodyne	0	f_B
Intradyne	IF $< f_B/2$	f_B
Heterodyne	IF $\geq f_B/2$	$\frac{3}{2}f_B$

A more recent example of this approach demonstrated the feasibility of using up to 1024 wavelength channels in the UDWDM configuration to provide 1 Gbit/s/λ over up to 100 km [9]. This was achieved by employing the advanced modulation format QPSK, which is twice as spectrally efficient as OOK. Because the receivers use a linear detection method, the signal could be digitized using analogue-to-digital converters (ADC) and equalized in the digital domain, recovering the state of polarization (SOP) such that an arbirary SOP could be launched into the fiber. The disadvantage of this approach is that, because the receiver is heterodyne, this requires ADCs that have a higher sampling frequency than the data rate (see Table I). Note, however, that proof-of-concept, realtime operation of this network has already been demonstrated [11]. It is only a small step from the polarization-diverse heterodyne coherent solution to a network based on phase- and polarization-diverse intradyne coherent receivers, which have an intrinsic 3 dB shot noise limited sensitivity gain over heterodyne receivers due to their measurement of the signal's quadrature component [12]. For intradyne coherent reception the frequency offset between the signal and LO is free to vary so long as the sum of the signal and beat frequencies remain within the sampling bandwidth; although in practice is limited by the algorithm chosen to track the frequency offset in the DSP. Again, a tunable LO laser can be used to select the channel of interest. Ordinarily, the ADCs in these receivers sample at twice the symbol rate (the Nyquist limit is 1 sample/symbol), resulting in reduced electrical bandwidth requirements when compared to heterodyne receivers. These electrical bandwidth requirements are further reduced when the cardinality of the modulation format is increased; for example, symmetric 10 Gbit/s/λ has been demonstrated over 100 km using PDM-QPSK at 3.125 GBd (requiring only 3.125 GHz receiver electrical bandwidth) [13]. As in the heterodyne case, equalization can be applied through the use of adaptive linear digital filters [14]. The downside to this receiver is the optical complexity; requiring a dual-polarization 90° optical hybrid to separate the in-phase and quadrature signal components (which is not required for heterodyne receivers), and at least four photodiodes and ADCs (compared to two for heterodyne).

Phase- and polarization-diversity has previously been explored in the context of receiver sensitivity in [15], where it was shown that a homodyne receiver's sensitivity was directly related to the power of the LO laser, but fundamentally limited by shot noise. This principle applies equally to heterodyne and intradyne receivers, although intradyne receivers have a 3 dB shot noise limited sensitivity gain over heterodyne receivers. It was also shown here that polarization multiplexing does not affect receiver sensitivity (however, it does reduce transceiver bandwidth requirements). It is a key advantage of all coherent receivers that the coherent gain (and therefore their sensitivity) can be improved by simply increasing LO power; an option not available to direct detection receivers.

Of the LR-PON architectures investigated to date, networks based on heterodyne or intradyne coherent receivers offer the highest data rate per subscriber while being scalable and reconfigurable, although these advantages come at the expense of increased optical complexity. In the case of a digital coherent receiver, some optical complexity can be transferred to the digital domain, and examples are provided later in this paper where we consider the benefits and challenges of an access network based on phase- and polarization-diverse digital coherent receivers.

III. PROPOSED NETWORK ARCHITECTURE

Previously, we proposed an architecture (see Fig. 2) which takes advantage of digital coherent receivers in order to enable, under ideal circumstances, high capacity (10 Gbit/s/λ), long reach (up to 100 km) and a high split ratio (up to 1:1024) [16]. In practice, there are constraints which can restrict the achievable receiver sensitivity and therefore split ratio. In this section we elucidate the details of this architecture, showing where these constraints arise and how they can be overcome.

A. Downstream

The downstream signal path can be divided into four elements: UDWDM signal generation and modulation in the OLT, transmission over single mode fiber (SMF) backhaul, 1:M passive split, and coherent reception in the ONU. The UDWDM

comb contains M carriers such that each ONU communicates on a dedicated wavelength channel.

Each ONU receives every channel because the midspan split is both passive and transparent to channels in the C-band. Note that the absence of filters in the schematic is deliberate; as previously noted, the LO laser in each ONU can be tuned to match the downstream channel of interest and reject the adjacent channels through coherent gain of the channel of interest. The obvious advantage of this configuration is that it limits the required inventory for the network (i.e., every ONU is identical). A further advantage is that multiple ONUs can be placed at each access point to provide high bandwidth fiber backhaul (e.g., for wireless applications).

It should be noted that the colorless network architecture impacts heavily on loss budget. The passive split, alone, incurs a minimum $10\log_{10}(M)$ dB loss, while the fiber backhaul incurs a typical loss of 0.2 dB/km (SMF). Some of this loss can be overcome by increasing the launch power to the fiber, and per channel powers of 8 dBm have been shown to be practical in a 5-channel UDWDM scenario [13], however, it was also shown that such high powers will necessarily restrict the total number of channels, in part due to nonlinear signal distortions. While the transmission distance is only 100 km, the low symbol rate, large number of channels and high channel power could excite nonlinearity in the form of cross-phase modulation [17]. It is also important that the total optical power is kept low enough to avoid fiber damage; for example, the fiber fuse effect has been demonstrated in SMF with optical powers of 31.5 dBm [18].

The total optical bandwidth available in the C-band is 5 THz. Assuming a target downstream comb of $\sim$1000 wavelengths, the channel spacing would necessarily be 5 GHz [16]. However, for reasons of risk management, it is unlikely that operators will use all the capacity of a single fiber. In this case, operation could be supported with up to 500×10 GHz spaced channels for the downstream and an additional 500 channels for the upstream. Feasibility studies have confirmed that bidirectional operation is possible without penalty [13].

B. Upstream

In many respects, the upstream signal path is actually less complicated than the downstream counterpart: each ONU transmits a single modulated wavelength, the signal is passively combined with the upstream channels from other ONUs, the signals co-propagate through the SMF backhaul and are detected by a bank of coherent receivers in the OLT. If the coherent receivers used in the OLT have sufficient optical/electrical bandwidth, then each receiver can detect multiple upstream channels. This reduces the number of receivers required and therefore lowers the complexity of the OLT.

Fiber nonlinearity is unlikely to impact upstream transmission as, throughout the distribution section of the network, there is only a signal channel. Due to the passive combiner, this channel sees $10\log_{10}(M)$ dB loss, meaning that even with multiple co-propagating channels, four-wave mixing products are unlikely to be excited due to the low total optical power. Based on these assumptions, the loss budget of the upstream channels would be equal to or greater than the downstream channels.

However, this is not the case with bidirectional transmission, where reflections from the upstream signal path could re-enter the ONU and interfere with the downstream signal, effectively leading to in-band noise accumulation[2]. This can be partly overcome by adopting the frequency plan shown in Fig. 2. Here, the LO laser is shifted to a higher frequency using single-sideband modulation (in this case 5 GHz higher than the downstream wavelength), before transmission. Reflected power then enters the ONU coherent receiver as an additional channel, and is rejected by the coherent receiver, even if the reflected power is much greater than the signal power [19]. In this way, only a single tunable laser is required for the LO and signal, and the upstream frequency grid is set automatically from the downstream comb.

When tuning to select a downstream channel, the laser may produce several spurious wavelengths within the switching time. To prevent interference with other channels, the output of the laser must be switched off. The method depends on the laser used however, for the laser described in the following subsection, this would involve reverse biasing the semiconductor optical amplifier on the output of the device during a switching event (also known as blanking [20]).

C. Tunable Laser

In order for the network and receiver to be truly colorless, the ONUs must incorporate C-band tunable LO and signal lasers (as previously noted, one tunable laser per ONU is sufficient). External cavity lasers (ECL) are one such source which could be employed however, while they generally exhibit low linewidths, they present issues in terms of cavity stability [21] and large form factor. Crucially, for an access network, their manufacture has not been demonstrated using a scalable production process so it is unlikely that they could be produced inexpensively.

Semiconductor lasers, such as the digital supermode distributed Bragg reflector (DS-DBR) laser, are an example of a more cost-effective C-band tunable laser, which are suitable for mass production [22]. The disadvantage of such lasers is that noise on electrical driving circuitry can be translated into the optical domain leading to RIN and frequency (1/f) noise (in addition to the intrinsic cavity linewidth) [23]. This can also lead to issues of amplitude and frequency instability (see Section V). Nevertheless, if these issues can be overcome then semiconductor lasers offer great potential for coherent access networks.

In this work, we make use of a DS-DBR laser, which is a commercially available, monolithically integrated, multisection, semiconductor laser. While the laser is C-band tunable, it has been designed to tune on a 50 GHz grid [24]; otherwise it is typical of a light source required for coherent PON applications. The experimental work detailed herein aims to show the applicability of such a device by measuring receiver sensitivity across several 10 GHz spaced channels, selected by a combination of electrical and thermal tuning (see Section IV).

The Lorentzian linewidths of the two DS-DBR lasers used in this investigation were measured using a coherent heterodyne technique with digital analysis [25]. The reference laser used when measuring linewidth was an ECL (linewidth $\sim$200 kHz). These results are shown in Fig. 3.

[2]Note that reflections present a greater challenge in the ONU due to limited resources. Optical filters could be applied at the OLT to mitigate backreflections. Alternatively, a dual fiber backhaul could be deployed, as in [7].

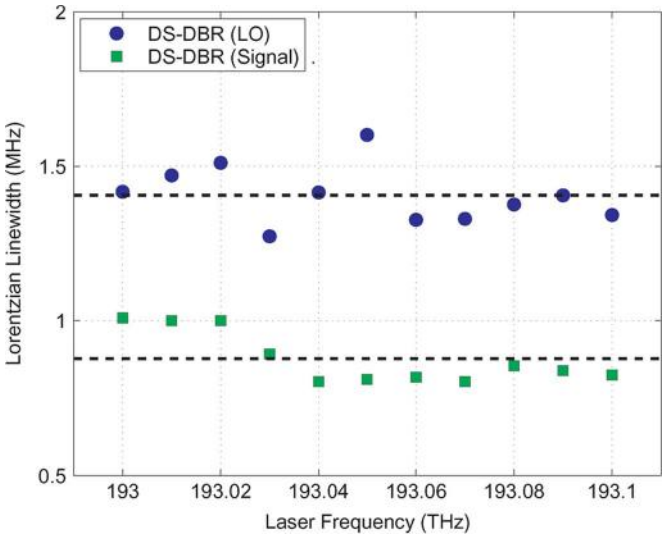

Fig. 3. Phase noise measurement of the two DS-DBR lasers used in this work. The phase noise is defined here as the convolution between the Lorentzian component of the DS-DBR and ECL linewidths. (ECL linewidth ∼200 kHz.) The mean linewidth (horizontal dashed lines) for the LO laser was 1.4 MHz, and 880 kHz for the signal laser.

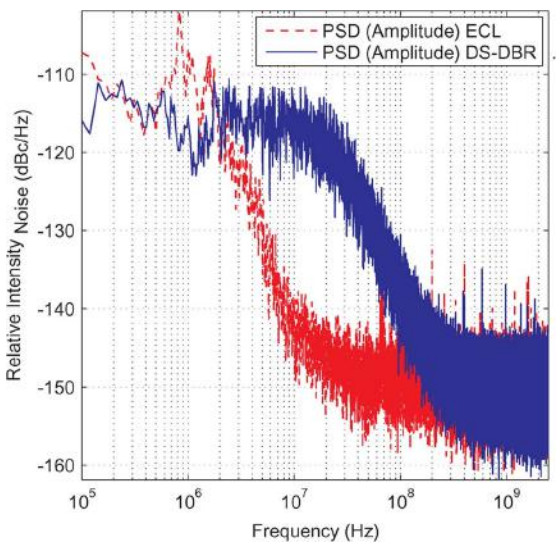

Fig. 4. Self-homodyne RIN spectrum measurement of a DS-DBR laser and an ECL.

The RIN of the lasers used as local oscillators was also measured using a self homodyne coherent technique. Here, the power spectral density of the signal was analyzed digitally to provide an estimate of the RIN spectrum; this approach enables the measurement of RIN over a large bandwidth and at low frequencies. Due to the challenges associated with removing the noise floor from the measurement, we were not able to estimate the absolute RIN of each laser using this technique. However, we were able to reference the RIN spectrum of these lasers to separate RIN measurements taken at high frequencies using a network analyzer, which automatically removes the noise floor from each measurement. The combined result of these approaches is in line with manufacturer specifications, and presented in Fig. 4.

IV. Experimental Configuration

To demonstrate the feasibility of a coherent LR-PON incorporating DS-DBR lasers, we implemented a single-channel version of the downstream link of the architecture described in Section III. This experimental configuration (shown in Fig. 5) involved the generation, transmission and detection of 3 GBd (12 Gbit/s) polarization division multiplexed (PDM) quadrature phase shift keying (QPSK).

While the laser was the main CW light source used in this work, these experiments were also undertaken using an ECL (linewidth ∼200 kHz) as an ideal reference.

The QPSK signal was generated by modulating CW light from a DS-DBR laser using a nested Mach-Zehnder modulator (denoted 'IQ Mod.') driven with two decorrelated $2^{15} - 1$ pseudo-random binary sequences (PRBS). Emulation of polarization multiplexing was achieved by splitting the optical signal into two arms of a passive delay line stage. The two arms were decorrelated by 152 symbols before recombination in orthogonal polarizations using a polarization beam combiner.

To emulate the LR-PON fiber backhaul, the PDM-QPSK signal power was set to 0 dBm and transmitted over 100 km standard single mode fiber (SMF). The total fiber attenuation was 20 dB (0.2 dB/km) with a chromatic dispersion at 1550 nm of 17 ps/nm/km. Splitting loss (assumed hereafter to be an ideal 3 dB loss per 1:2 split) was also emulated by using a variable optical attenuator between the fiber and the coherent receiver.

The phase- and polarization-diverse coherent receiver combines the signal and LO in orthogonal polarization states using a polarization beam splitter. A 90° optical hybrid (in each polarization) was used to introduce a phase shift between signal and LO such that both the in-phase and quadrature components of the signal could be recovered. The beat signal was detected using four balanced photodiodes and digitized using a digital storage oscilloscope incorporating four ADCs operating at 50 GSa/s. The digitized signal was downsampled to 2 samples/symbol (6 GSa/s) and processed offline using parallel DSP (see Section V).

Note the assumption that hard decision forward error correction (FEC) could be applied such that the 20% coding overhead (2 Gbit/s) would enable correction of a BER up to 1.1×10^{-2} to below 10^{-15} [26]. We further note, for completeness, that hard decision FEC algorithms have been documented which would enable the correction of BER up to 1.5×10^{-2} [27], and beyond for soft decision algorithms [28]. While the achievable net coding gain for a fixed computational complexity is likely to improve in the near future, in this work the FEC limit was set as a realistic compromise between performance and complexity.

Each tuning section of the DS-DBR lasers was driven using arbitrary waveform generators (ArbWG). The DS-DBR laser has been designed to tune to a 50 GHz grid, so fine resolution wavelength adjustments were achieved using temperature controllers. Although this is a single channel investigation, the relevance of this configuration to a colorless UDWDM PON was highlighted by measuring the receiver sensitivity across 11×10 GHz spaced channels (193.0–193.1 THz) by retuning both signal and LO lasers.

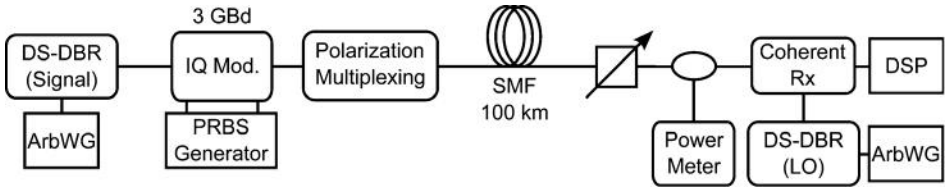

Fig. 5. Experimental Configuration for measuring receiver sensitivity with DS-DBR lasers for signal and LO.

V. Digital Signal Processing

Experimentally, we can apply DSP offline in order to evaluate the performance of realtime processing; for example, here we have used 50 GSa/s ADCs and digitally downsampled to 6 GSa/s. For realtime processing, four receiver ADCs operating at 2 Sa/symbol would each capture data at 6 GSa/s, with a total throughput of 24 GSa/s. The high symbol rates encountered in optical communications would present a challenge for chip design if all the data were to be processed serially. However, applying serial-to-parallel converters on the output of the ADCs produces a fixed-width bus of samples which can be processed at a fraction of the total sample rate. Here, we detail key elements used for parallel DSP, and provide an estimate for the required clock frequency of an application-specific integrated circuit (ASIC). In order to accurately emulate realtime processing, the offline DSP used in this experiment is also parallelized.

The DSP comprises four main elements: serial-to-parallel conversion, normalization of the input signal from each ADC to unit power, equalization (primarily for tracking polarization rotations, however this also enables symbol retiming and residual chromatic dispersion compensation) and differential carrier recovery.

The equalization was applied using a parallel implementation of the constant modulus algorithm (CMA) [29], consisting of 5 complex taps applied in parallel across a full bus width. The tap weights were updated using a least mean squares (LMS) algorithm calculated using the mean of the error terms obtained for each bus; this averaging approach is more robust to noise than the serial CMA [30]. The equalizer taps were initialized using the scheme outlined in [31] before applying equalization on a bus-by-bus basis, with the filter taps being updated at the end of each bus. In practice, we found that bus width had only a minor influence on sensitivity, and so opted for a 128 sample bus, corresponding to a 46.9 MHz update rate.

Based on linewidth measurements of the DS-DBR lasers given in Section III, it would not be possible to apply carrier phase estimation without incurring a penalty [32]. Experimentally, it was found that for signals affected additionally by the RIN from the LO (see Section V.B) Viterbi and Viterbi carrier phase estimation did not produce an accurate phase estimate. Therefore, we differentially decode each symbol by comparing the equalized fields of adjacent symbols, and details of the algorithm are given in V.A.

Section III also highlights the RIN spectrum of DS-DBR lasers. This can been compensated as part of the normalization block, and the theory and implementation of this method are given in V.B.

A. Phase and Frequency Offset Compensation

The linewidth·symbol-time product ($\Delta\nu\tau_s$) determines both the efficacy and feasibility of carrier phase estimation, assuming that phase estimation is performed only once per symbol [32]. Even with the low symbol-rates considered here, $\Delta\nu\tau_s$ can be $<10^{-4}$ when using an ECL at the transmitter and receiver. This permits the use of the Viterbi and Viterbi fourth power phase estimation algorithm, which is detailed in [33]. Conversely, with a DS-DBR laser at the transmitter and receiver, $\Delta\nu\tau_s$ is approximately $\sim 8 \times 10^{-4}$. The high resulting phase noise means that using fourth power phase estimation results in repeated cycle slips whereby a succession of incorrect phase estimates lead to a $(\pi/2)$ deviation from the actual phase, invalidating subsequent data.

Differential decoding by symbol (DS) and differential detection by field (DF) can be used to overcome cycle slips. In both cases, data is encoded on the difference between the phase of two adjacent symbols. At the receiver this data is recovered by comparing the phase of two consecutive received symbols. DS involves making a decision on the symbol before differentially decoding, and therefore requires carrier phase estimation.

DF is used in this work, which is a digital implementation of the interferometric approach applied in optical DQPSK experiments. By first digitizing the signal, equalization can be applied, making this approach more robust to chromatic dispersion and mismatched optical path lengths within the receiver while permitting polarization multiplexing without optical polarization tracking. Additionally, a high-power LO laser can be used, which can improve receiver sensitivity [15]. In this scenario, the carrier phase is not directly recovered, but inferred from the difference between two symbols.

$$\begin{aligned} r_s r_{s-1}^* &= e^{j(\frac{\pi}{2}M_{s-1})} e^{-j(\frac{\pi}{2}M_s+\omega\tau_s)} \\ &= e^{-j(\frac{\pi}{2}M_s-\frac{\pi}{2}M_{s-1}+\omega\tau_s)} \end{aligned} \quad (1)$$

where r_s is a symbol from the equalized symbol stream, $M_s \in 0\ldots3$ is the encoded data on symbol s, and $\Delta\omega$ is the angular offset between two adjacent symbols. The result of $\Delta\omega$ is that any frequency offset will lead to a fixed rotation of the QPSK constellation points. To calculate the frequency offset from this result, the data must be removed using a fourth power operation. In practice, the frequency offset estimate is derived from a noisy signal so the angle of a multiple symbol average can be taken as follows.

$$\begin{aligned} \frac{1}{4}\angle\left(\sum_{s=-n}^{n}\left[r_s r_{s-1}^*\right]^4\right) &= \frac{1}{4}\angle e^{-j(4\omega\tau_s)} \\ &= -\omega\tau_s \end{aligned} \quad (2)$$

where the window length is $2n + 1$. This is analogous to the Viterbi and Viterbi algorithm, but without the requirement of phase unwrapping (this has already been applied differentially).

Note that, even when the frequency offset is relatively small, this estimation performs two important functions. Firstly, this algorithm can track small changes in the frequency offset over time; this relaxes the constraints on the frequency stability of the LO laser. Crucially, however, from an implementation perspective, this provides a metric to feed back to the LO laser itself to ensure that the frequency offset from the signal is kept small.

In the case of DS, frequency offset estimation and carrier recovery are applied before a hard decision on the symbol is made; only then is differential decoding applied. DS, while less tolerant to phase noise than DF, avoids the additional SNR penalty due to the multiplication of noise terms from two adjacent symbols. Due to the duplication of errors (an error in one symbol will lead to an error in the next symbol), in an additive white Gaussian noise (AWGN) channel with high OSNR, both methods will at least double the BER [32].

B. Time-Dependent DC Offset Removal

Intrinsic RIN poses a challenge for all sensitivity-limited receivers. In the case of IM-DD, it may be obvious that RIN will degrade SNR, but the impact on coherent phase-modulated communications systems is not so clear.

A recent theoretical investigation into the impact of RIN on digital coherent receivers showed that LO lasers affected by RIN degrade power sensitivity [34]. Coherent receivers using balanced photodiodes with infinite common mode rejection ratio (CMRR) are immune to this translation of intensity noise into the digital domain though, in practice, differential amplification is not ideal (finite CMRR).

It has previously been shown that, under certain circumstances, RIN can be partially compensated digitally [35]. This is in direct contrast to the particularly effective optical approach for RIN reduction [36], [37]. Unfortunately, the optical approach is beyond the permissible complexity for an ONU, and so the digital approach is a reasonable compromise.

Here, the theoretical basis for RIN compensation is outlined. The RIN of a laser is defined as the ratio of the mean-square optical intensity fluctuation, normalised to a 1 Hz bandwidth at a fixed frequency, and the average optical power. When a laser with non-negligible RIN spectrum is used as the LO laser, the intensity noise will contribute to the beating between LO and signal. This RIN component can be treated as an additional electric field without loss of generality and so, neglecting extrinsic noise sources, this leads to the following signal from the photodiodes

$$\begin{aligned} I_+ &\propto |E_{\mathrm{Sig}} + (E_{\mathrm{LO}} + E_{\mathrm{RIN}})|^2 \\ I_- &\propto |E_{\mathrm{Sig}} - (E_{\mathrm{LO}} + E_{\mathrm{RIN}})|^2 \end{aligned} \tag{3}$$

where $E_{\mathrm{Sig,LO,RIN}}$ are the electric fields corresponding to the signal, LO and RIN, respectively, and $I_{+,-}$ are the electric currents from the two square-law photodiodes comprising the balanced photodector. These signals are passed to differential amplifiers (with a finite CMRR) resulting in the final output current

$$\begin{aligned} I \propto\ & 2C(E_{\mathrm{LO}}E_{\mathrm{Sig}} + E_{\mathrm{RIN}}E_{\mathrm{Sig}}) \\ & +(1-C)\left(E_{\mathrm{LO}}^2 + E_{\mathrm{Sig}}^2 + E_{\mathrm{RIN}}^2 + 2E_{\mathrm{LO}}E_{\mathrm{RIN}}\right) \end{aligned} \tag{4}$$

where $C/(1-C)$ is the CMRR, and C is normalized to unity $(0 < C < 1)$. Assuming that E_{RIN} and E_{Sig} are both small compared with E_{LO}, then terms including E_{LO} will dominate

$$I \propto 2C(E_{\mathrm{LO}}E_{\mathrm{Sig}}) + (1-C)(2E_{\mathrm{LO}}E_{\mathrm{RIN}}) \tag{5}$$

where constant terms have been removed due to the assumed AC-coupling of the receiver. As the amplitude of E_{LO} increases relative to E_{Sig}, the relative amplitude of $E_{\mathrm{LO}}E_{\mathrm{RIN}}$ also increases. With a finite CMRR, and assuming that E_{RIN} varies with Gaussian statistics, this introduces an LO-RIN beat term which cannot be removed. However, RIN from a semiconductor laser is normally manifested as 1/f noise (or 'pink noise') due mainly to noise from driving circuitry being translated into the optical domain [23]. For the DS-DBR laser this results in the RIN spectrum shown in Fig. 4.

Since the RIN spectrum is not white, we can use (5) to design a digital filter which tracks changes in amplitude over time and, in this respect, the obvious choice is an averaging window, which treats $|E_{\mathrm{LO}}E_{\mathrm{RIN}}|^2$ as a time-dependent DC offset[3]. This can be applied to the signal from each channel as a finite impulse response filter (FIR) in the time domain, where the filter coefficients are given by

$$x[n] = \begin{cases} 1 - 1/N & \text{if } n = N/2 \\ -1/N & \text{otherwise.} \end{cases} \tag{6}$$

Here, N is the number of filter taps, which is set depending on the signal-LO ratio, the RIN spectrum of the LO laser, and the CMRR of each channel. Note that other filters can be designed with a high pass characteristic (such as a Gaussian filter) which should also compensate for RIN, however the complexity would be greater than for the filter proposed here.

C. Serial vs. Parallel DSP Performance

Previously, we have reported results from proof-of-concept experiments, where DSP had been applied to the received signals offline and serially (for example [16]). In this context, the key difference between serial and parallel processing is the CMA update rate. In the serial case, the equalizer taps are updated on a symbol-by-symbol basis, but for the parallel case this update is applied on a bus-by-bus basis; effectively averaging the CMA error over multiple symbols.

We compare the serial and parallel DSP algorithms in Fig. 6 in order to validate previous results[4]. The first analysis, Fig. 6(a), shows the receiver sensitivity when using an ECL laser at the transmitter and the receiver. It is clear that, in this scenario, the bus width has no impact on receiver sensitivity. Fig. 6(b) shows the results from the same investigation when the ECLs are replaced by DS-DBR lasers. Even with the reduced coherence time for these lasers (Fig. 3), there is still a negligible impact on sensitivity when moving from serial DSP to parallel DSP with a bus width up to 1024 samples. Note that the feedback time for the CMA error term is the (symbol time)·(bus width) product.

[3]The implicit assumption here is that the receiver is AC coupled such that $\langle I \rangle = 0$.

[4]It should be additionally noted that for reasons of expedience, the results shown in the Appendix, as well as in Fig. 7 are processed using optimized serial DSP. The results in Fig. 6 validate this approach.

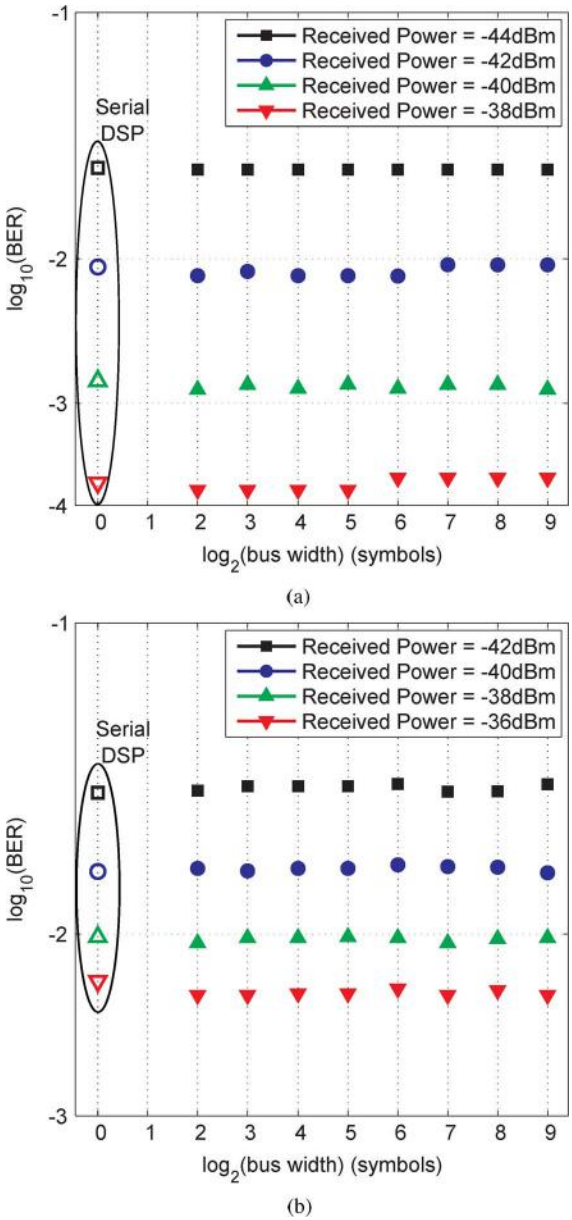

Fig. 6. Impact of bus width on receiver sensitivity. Open markers indicate performance using serial processing for each optical power level. The difference in BER between serial and parallel DSP algorithms is negligible, and independent of the laser used. (a) ECL LO, ECL signal, (b) DS-DBR LO, DS-DBR signal.

VI. Results and Discussion

In this paper, we have outlined some potential challenges associated with the use of tunable semiconductor lasers for low symbol-rate, sensitivity-limited coherent communications; namely RIN and linewidth. In this section, we detail an experimental characterization of the RIN compensating filter introduced in Section V.B. We then apply these results to a transmission system outlined in Section IV while using parallel DSP at the receiver.

A. RIN Compensation

It was suggested in [34] and also by the analysis in Section V that, for a receiver with finite CMRR, there would be a penalty due to laser RIN. With a high LO-signal ratio, RIN from the LO laser would be enhanced and would therefore reduce the sensitivity of a coherent receiver. The (low power) RIN from the signal laser would have a minimal impact on receiver sensitivity. The impact of RIN is dependent on the CMRR, which was measured to be between 10 dB and 15 dB for all four channels (signal and LO port) of the coherent receiver used in these investigations. Results are shown in Fig. 7 from a back-to-back performance characterization of achievable receiver sensitivity when incorporating a digital RIN compensating filter within the receiver DSP. Here, we have extrapolated the required sensitivity at the FEC limit, however the complete data are shown in the Appendix. To obtain these results, four combinations of the two laser types were investigated (DS-DBR and ECL as signal or LO).

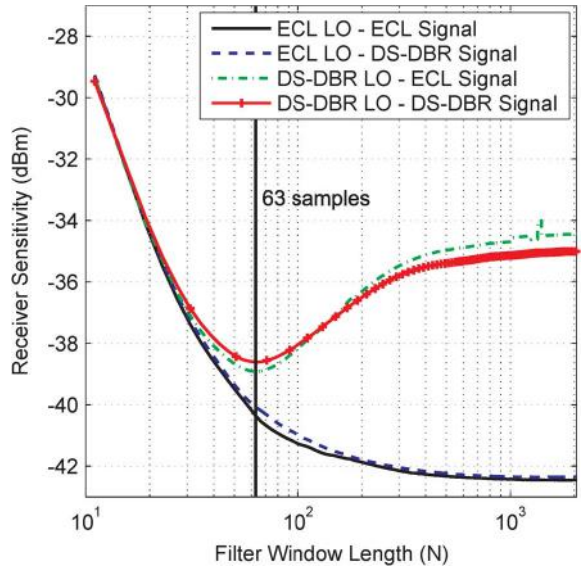

Fig. 7. The required received power to achieve a BER below the FEC limit (1.1×10^{-2}) for different RIN compensation filter window sizes. The vertical line indicates the filter length that optimizes receiver sensitivity. (These results are obtained by fitting received power against Q^2-factor.).

When ECLs are used as both the signal and LO lasers, the receiver sensitivity improves asymptotically with increasing length of the RIN compensating filter window; up to the maximum filter length tested (2049 taps). This indicates that the DC offset of the coherently detected signal is approximately time invariant over this interval. Conversely, when DS-DBR lasers are used as the signal and LO sources, there is a particular window length which optimizes filter performance for each received power, implying that low-frequency noise has been removed.

The final two curves show the performance when an ECL and DS-DBR laser are used as the signal and LO source, or LO and signal source, respectively. A comparison of these results confirms the theory that it is RIN from the LO laser that impacts on receiver sensitivity.

B. Transmission Performance

The results in this section were obtained using the experimental configuration shown in Fig. 5, including transmission over 100 km SMF. Shown in Fig. 8 is the measured receiver

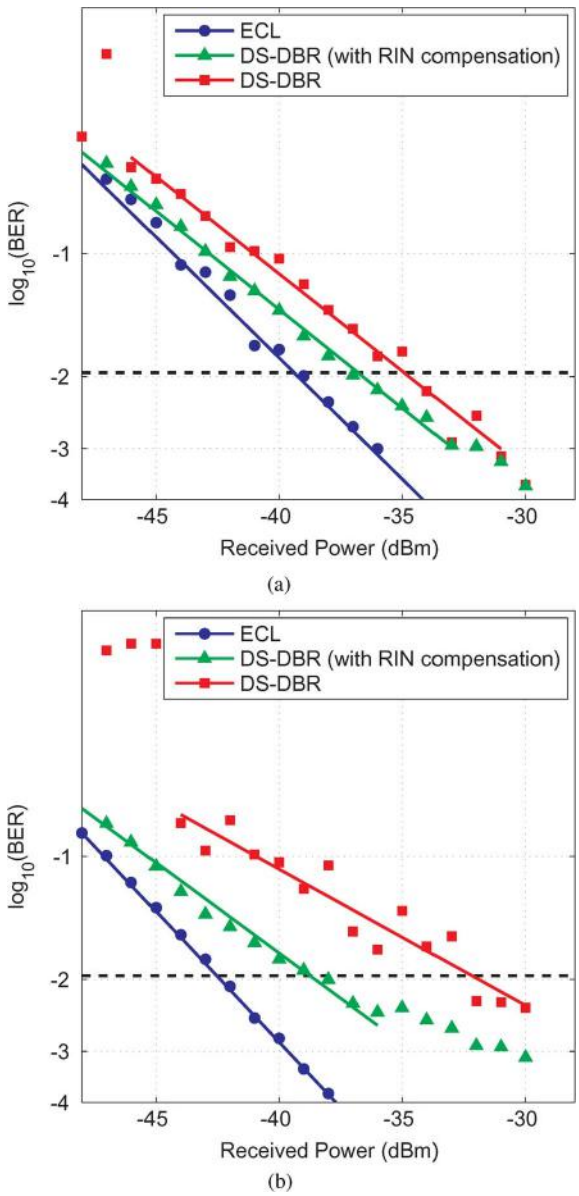

Fig. 8. Experimentally determined receiver sensitivity of 3 GBd PDM-QPSK after transmission over 100 km SMF. Shown is the sensitivity of the first channel (193 THz) with and without digital RIN compensation (dashed horizontal line is the 1.1×10^{-2} BER limit for FEC). (a) 10 dBm LO Power, (b) 15 dBm LO Power.

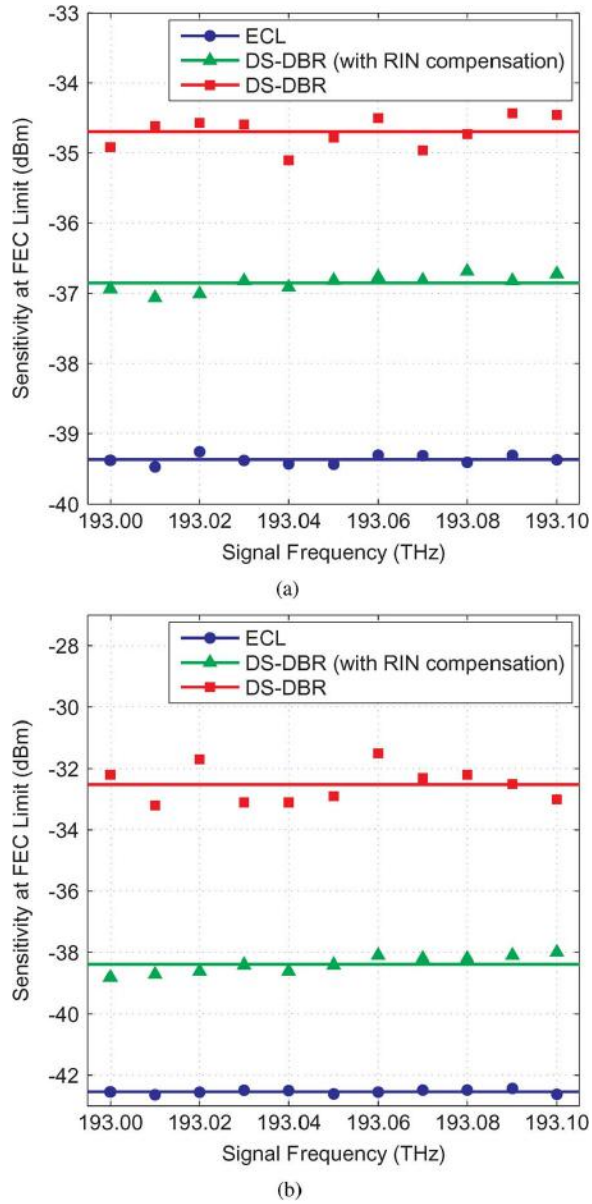

Fig. 9. Individual channel sensitivities, with the horizontal lines indicating the average sensitivity for each configuration. The receiver sensitivity when using ECLs is shown as a reference. (a) 10 dBm LO Power, (b) 15 dBm LO Power.

sensitivity when using DS-DBR lasers at the transmitter and receiver tuned to 193 THz. The BER degrades significantly when the LO-signal ratio is around 60 dB due to the increased impact of RIN. We found that, in the low signal power region, LO RIN lead to equalizer false locking (discarding data from one polarization) or malconvergence, leading to significant BER degradation.

When RIN compensation was applied the receiver sensitivity improves, albeit with an error floor at higher powers. It is evident that there is an error floor when no RIN compensation is applied, so we attribute the error floor in this case to the incomplete removal of RIN. The performance when using ECLs is shown for reference, and the relative penalty at the FEC limit is 3.7 dB. The achievable sensitivity for the DS-DBR configuration is -38.8 dBm, when using an LO power of 15 dBm.

Fig. 9 shows how receiver sensitivity varies when changing the operating frequency of the DS-DBR lasers. We found that, when RIN compensation was applied, the variance of receiver sensitivity was negligible, indicating the suitability of this approach for UDWDM-PON. In Fig. 9(a), the LO power was set to 10 dBm and for Fig. 9(b) it was set to 15 dBm. Comparing these results further confirms the theory that a higher LO power increases the impact of LO RIN, while also showing the enhanced efficacy (and necessity) of RIN compensation. For a 10 dBm LO power, the average sensitivity improvement at the FEC limit when applying RIN compensation was 2.1 dB, while for a 15 dBm LO power this increased to 5.9 dB.

We now make several observations which place these results in the context of previous work. Firstly, the improved receiver

sensitivity in Fig. 9(a) when compared with the results reported in [35] is due to the redesigned frequency offset tracking outlined in Section V.A (the previous implementation used a feedback algorithm which introduced an error floor). Second, these results can be used as a basis for estimating network performance. Assuming 5 dBm/λ launch power [13], the loss budget for a 10 dBm (15 dBm) LO power is 41.9 dB (43.4 dB). For the configuration outlined in Section III, assuming 3 dB loss per 1:2 split, this loss budget would enable transmission over 100 km with a 1:128 (1:128) way split (albeit with a 2.4 dB margin in the latter case). The aggregate network capacity in this configuration would be 1.28 Tbit/s. The total optical power at launch would be 26 dBm; comparable to the output power of a high-power EDFA.

VII. Conclusion

We have provided a summary of state-of-the-art WDM-LR-PON architectures, and shown how the use of coherent detection enables high capacity and high split ratios. In particular, we have discussed how a tunable LO laser can be used to select a channel from a UDWDM source, removing the need for complex optical filtering while providing a scalable, reconfigurable network.

The tunable LO was chosen to be a DS-DBR semiconductor laser, which is fully C-band tunable. It was shown theoretically and experimentally that the enhanced linewidth and RIN from these lasers (relative to an ECL) could be tolerated using digital postprocessing of the received signal and that, without RIN compensation, equalizer convergence could not be guaranteed. It was shown experimentally and theoretically that, in contrast to the signal laser, RIN from the LO laser degrades receiver sensitivity.

The DSP was implemented using a parallel structure to demonstrate the potential for future implementation and realtime operation on an ASIC. It was shown that the parallel processing bus width does not impact on receiver sensitivity.

The receiver sensitivity of 3 GBd (12 Gbit/s) PDM-QPSK was measured across 11×10 GHz spaced channels. Receiver sensitivity was measured in two configurations: using ECLs for signal and LO sources (ideal case), and using DS-DBR lasers for signal and LO sources. It was found that, when using an LO power of 10 dBm (15 dBm), the average receiver sensitivity in the ideal case was -39.4 dBm (-42.5 dBm), at the 1.1×10^{-2} BER limit for FEC, dropping to -36.9 dBm (-38.4 dBm) when using DS-DBR lasers with RIN compensation. Using DS-DBR lasers without digital RIN compensation lead to equalizer malconvergence and degraded receiver sensitivity by a further 2.2 dB (5.9 dB).

Through a brief analysis, we show that a network based on digital coherent receivers and DS-DBR lasers could theoretically support 128×10 Gbit/s channels.

Appendix

Fig. 7 shown in Section VI.A is an extrapolated result, which demonstrates that digital RIN compensation need only be applied if the LO laser exhibits a high relative intensity noise (RIN from the signal laser has a negligible impact on performance). Shown here, for completeness, are the original plots

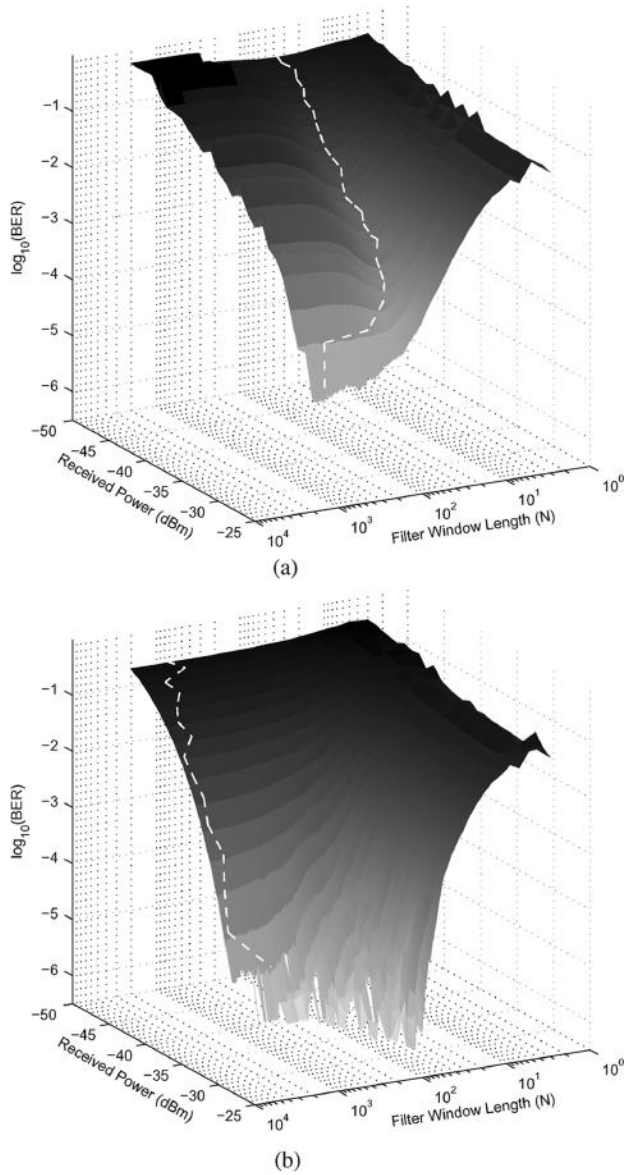

Fig. 10. Relationship between BER, received power and the length of the RIN compensating filter window for 3 GBd PDM-QPSK when using (a) DS-DBR lasers as signal and LO sources and (b) ECLs as signal and LO sources. The white dashed line indicates the minimum BER for each received power. (a) DS-DBR Signal, DS-DBR LO, (b) ECL Signal, ECL LO.

which show the sensitivity after RIN compensation with different filter lengths. Fig. 10(a) shows the impact of RIN compensation when a DS-DBR laser is used as the LO laser. The RIN compensation filter is found to be most efficacious for low signal powers (high LO-signal ratio), and the 3 dB response of this high pass filter tends to $\sim$100 MHz in this region. It was shown in Fig. 4 that the intensity noise of the unmodulated DS-DBR laser light was greatest below 100 MHz; corroborating this result.

For the case of a low-RIN LO laser (in this case, an ECL) the result is quite different, with the optimum filter cutoff frequency at high LO-signal ratio an order of magnitude lower ($\sim$10 MHz). This, too, is the expected result from the RIN spectrum measured in Fig. 4.

ACKNOWLEDGMENT

The authors extend their thanks to Oclaro Inc. for the supply of the DS-DBR lasers used in this work.

REFERENCES

[1] D. Shea and J. Mitchell, "A 10-Gb/s 1024-way-split 100-km long-reach optical-access network," *J. Lightw. Technol.*, vol. 25, no. 3, pp. 685–693, Mar. 2007.

[2] *Gigabit-Capable Passive Optical Networks (GPON): Reach Extension*, Recommendation G.984.6, 2008, Telecommunication Standardization Sector Std..

[3] *Gigabit-Capable Passive Optical Networks (GPON): General Characteristics*, Recommendation G.984.1, 2008, Telecommunication Standardization Sector Std..

[4] Z. Al-Qazwini and H. Kim, "Symmetric 10-Gb/s WDM-PON using directly modulated lasers for downlink and RSOAs for uplink," *J. Lightw. Technol.*, vol. 30, no. 12, pp. 1891–1899, Jun. 2012.

[5] K. Y. Cho, U. H. Hong, S. P. Jung, Y. Takushima, A. Agata, T. Sano, Y. Horiuchi, M. Suzuki, and Y. C. Chung, "Long-reach 10-Gb/s RSOA-based WDM PON employing QPSK signal and coherent receiver," *Opt. Exp.*, vol. 20, no. 14, pp. 15 353–15 358, Jul. 2012.

[6] P. Ossieur, C. Antony, A. Clarke, A. Naughton, H.-G. Krimmel, Y. Chang, C. Ford, A. Borghesani, D. Moodie, A. Poustie, R. Wyatt, B. Harmon, I. Lealman, G. Maxwell, D. Rogers, D. Smith, D. Nesset, R. Davey, and P. Townsend, "A 135-km 8192-split carrier distributed DWDM-TDMA PON with $2 \times 32 \times 10$ Gb/s capacity," *J. Lightw. Technol.*, vol. 29, no. 4, pp. 463–474, Feb. 2011.

[7] P. Ossieur, C. Antony, A. Naughton, A. Clarke, H.-G. Krimmel, X. Yin, X.-Z. Qiu, C. Ford, A. Borghesani, D. Moodie, A. Poustie, R. Wyatt, B. Harmon, I. Lealman, G. Maxwell, D. Rogers, D. Smith, S. Smolorz, H. Rohde, D. Nesset, R. Davey, and P. Townsend, "Demonstration of a 32×512 split, 100 km reach, $2 \times 32 \times 10$ Gb/s hybrid DWDM-TDMA PON using tunable external cavity lasers in the ONUs," *J. Lightw. Technol.*, vol. 29, no. 24, pp. 3705–3718, Dec. 2011.

[8] H. Rohde, S. Smolorz, E. Gottwald, and K. Kloppe, "Next generation optical access: 1 Gbit/s for everyone," in *Proc. ECOC*, Sep. 2009, Paper 10.5.5.

[9] S. Smolorz, E. Gottwald, H. Rohde, D. Smith, and A. Poustie, "Demonstration of a coherent UDWDM-PON with real-time processing," in *Proc. OFC/NFOEC*, Mar. 2011, Paper PDPD4.

[10] S. Narikawa, H. Sanjoh, N. Sakurai, K. Kumozaki, and T. Imai, "Coherent WDM-PON using directly modulated local laser for simple heterodyne transceiver," in *Proc. ECOC*, Sep. 2005, Paper We3.3.2.

[11] H. Rohde, S. Smolorz, J. Wey, and E. Gottwald, "Coherent optical access networks," in *Proc. OFC/NFOEC*, Mar. 2011, Paper OTuB1.

[12] E. Ip, A. P. Lau, D. J. Barros, and J. M. Kahn, "Coherent detection in optical fiber systems: Erratum," *Opt. Exp.*, vol. 16, no. 26, pp. 21 943–21 943, Dec. 2008.

[13] D. Lavery, E. Torrengo, and S. Savory, "Bidirectional 10 Gbit/s long-reach WDM-PON using digital coherent receivers," in *Proc. OFC/NFOEC*, Mar. 2011, Paper OTuB4.

[14] S. J. Savory, "Digital filters for coherent optical receivers," *Opt. Exp.*, vol. 16, no. 2, pp. 804–817, Jan. 2008.

[15] K. Kikuchi and S. Tsukamoto, "Evaluation of sensitivity of the digital coherent receiver," *J. Lightw. Technol.*, vol. 26, no. 13, pp. 1817–1822, Jul. 2008.

[16] D. Lavery, M. Ionescu, S. Makovejs, E. Torrengo, and S. J. Savory, "A long-reach ultra-dense 10 Gbit/s WDM-PON using a digital coherent receiver," *Opt. Exp.*, vol. 18, no. 25, pp. 25 855–25 860, Dec. 2010.

[17] C. Behrens, R. Killey, S. Savory, M. Chen, and P. Bayvel, "Nonlinear transmission performance of higher-order modulation formats," *IEEE Photon. Technol. Lett.*, vol. 23, no. 6, pp. 377–379, Mar. 2011.

[18] A. Rocha, F. Domingues, M. Facao, and P. Andre, "Threshold power of fiber fuse effect for different types of optical fiber," in *Proc. ICTON*, Jun. 2011, Paper Tu.P.13.

[19] D. Lavery, C. Behrens, and S. J. Savory, "On the impact of backreflections in a bidirectional 10 Gbit/s coherent WDM-PON," in *Proc. OFC/NFOEC*, Mar. 2012, Paper OTh1F.3.

[20] R. Maher, D. S. Millar, S. J. Savory, and B. C. Thomsen, "SOA blanking and signal pre-emphasis for wavelength agile 100 Gb/s transmitters," in *Proc. OECC*, Jul. 2012, pp. 905–906.

[21] K. Piyawanno, M. Kuschnerov, M. Alfiad, B. Spinnler, and B. Lankl, "Effects of mechanical disturbance on local oscillators and carrier synchronization," in *Proc. OECC*, Jul. 2010, pp. 124–125.

[22] M. Wale, "Photonic integration challenges for next-generation networks," in *Proc. ECOC*, Sep. 2009, p. Paper 1.7.4.

[23] L. Coldren and S. Corzine, *Diode Lasers and Photonic Integrated Circuits*. New York: Wiley-Interscience, 1995.

[24] *Spectral Grids for WDM Applications: DWDM Frequency Grid*, Recommendation G.694.1, 2012, Telecommunication Standardization Sector Std..

[25] R. Maher and B. Thomsen, "Dynamic linewidth measurement technique using digital intradyne coherent receivers," *Opt. Exp.*, vol. 19, no. 26, pp. B313–B322, Dec. 2011.

[26] B. Li, K. Larsen, D. Zibar, and I. Monroy, "Over 10 dB net coding gain based on 20% overhead hard decision forward error correction in 100 G optical communication systems," in *Proc. ECOC*, Sep. 2011, Paper Tu.6.A.3.

[27] F. Chang, K. Onohara, and T. Mizuochi, "Forward error correction for 100 G transport networks," *IEEE Commun. Mag.*, vol. 48, no. 3, pp. S48–S55, Mar. 2010.

[28] T. Mizuochi, K. Ouchi, T. Kobayashi, Y. Miyata, K. Kuno, H. Tagami, K. Kubo, H. Yoshida, M. Akita, and K. Motoshima, "Experimental demonstration of net coding gain of 10.1 dB using 12.4 Gb/s block turbo code with 3-bit soft decision," in *Proc. OFC/NFOEC*, Mar. 2003, Paper PD21.

[29] D. Godard, "Self-recovering equalization and carrier tracking in two-dimensional data communication systems," *IEEE Trans. Commun.*, vol. 28, no. 11, pp. 1867–1875, Nov. 1980.

[30] R. Maher, D. Millar, S. Savory, and B. C. Thomsen, "Fast switching burst mode receiver in a 24-channel 112 Gb/s DP-QPSK WDM system with 240 km transmission," in *Proc. OFC/NFOEC*, Mar. 2012, Paper JW2A.57.

[31] B. C. Thomsen, R. Maher, D. S. Millar, and S. J. Savory, "Burst mode receiver for 112 Gb/s DP-QPSK with parallel DSP," *Opt. Exp.*, vol. 19, no. 26, pp. B770–B776, Dec. 2011.

[32] M. Taylor, "Phase estimation methods for optical coherent detection using digital signal processing," *J. Lightw. Technol.*, vol. 27, no. 7, pp. 901–914, Apr. 2009.

[33] A. Viterbi and A. Viterbi, "Nonlinear estimation of PSK-modulated carrier phase with application to burst digital transmission," *IEEE Trans. Inf. Theory*, vol. 29, no. 4, pp. 543–551, Jul. 1983.

[34] B. Zhang, C. Malouin, and T. J. Schmidt, "Design of coherent receiver optical front end for unamplified applications," *Opt. Exp.*, vol. 20, no. 3, pp. 3225–3234, Jan. 2012.

[35] D. Lavery, R. Maher, D. S. Millar, B. C. Thomsen, P. Bayvel, and S. J. Savory, "Demonstration of 10 Gbit/s colorless coherent PON incorporating tunable DS-DBR lasers and low-complexity parallel DSP," in *Proc. OFC/NFOEC*, Mar. 2012, Paper PDP5B.10.

[36] M. A. Newkirk and K. J. Vahala, "Large (14.5 dB) reduction of intensity noise from a semiconductor laser by amplitude-phase decorrelation," *Appl. Phys. Lett.*, no. 11, pp. 1289–1291, Mar. 1991.

[37] L.-S. Fock, A. Kwan, and R. Tucker, "Reduction of semiconductor laser intensity noise by feedforward compensation: Experiment and theory," *J. Lightw. Technol.*, vol. 10, no. 12, pp. 1919–1925, Dec. 1992.

Domaniç Lavery (S'09) received the M.S. degree in theoretical physics from the University of Durham, Durham, U.K., in 2009, specializing in particle theory.

He joined the Optical Networks Group at University College London (UCL) the following October to pursue the Ph.D. investigating the use of digital coherent transceivers in the field of optical communications. His doctoral research focusses on the implementation and characterization of coherent-enabled advanced modulation formats and their application to spectrally efficient, high capacity passive optical networks.

Mr. Lavery was awarded the IEEE Photonics Society Graduate Student Fellowship in 2012. He is an associate member of the institute of physics (IOP), and has previously acted as a reviewer for IEEE publications.

Robert Maher (S'05–M'09) received his B.Eng. and Ph.D. degrees in electronic engineering from Dublin City University, Ireland, in 2005 and 2009, respectively.

His doctoral research focused on the development and characterization of cost efficient wavelength tunable transmitters suitable for reconfigurable agile optical networks. In 2009 he took up a position as a Postdoctoral Researcher within the Research Institute for Networks and Communications Engineering (RINCE), based in Dublin City University, where he carried out research on optical comb generation and coherent optical networks. In 2010 he was awarded an IRCSET INSPIRE Marie Curie Fellowship and joined the Optical Networks Group at University College London (UCL), U.K. His current research focuses on the characterization of fast switching semiconductor tunable lasers and dynamically reconfigurable burst mode coherent optical networks.

Dr. Maher is a member of the Marie Curie Fellows Association (MCFA) and is a reviewer for IEEE PHOTONICS TECHNOLOGY LETTERS.

David S. Millar (S'07-M'11) was born in Manchester, U.K., in 1982. He received the M.Eng. degree in electronic and communications engineering from the University of Nottingham, Nottingham, U.K. in 2007, and the Ph.D. degree in optical communications from University College London (UCL), London, U.K. in 2011.

He is currently working at Mitsubishi Electric Research Labs in Cambridge, MA, USA. His research interests include coherent optical transmission systems, digital coherent receiver design, DSP techniques for advanced modulation formats, and digital nonlinearity mitigation.

Dr. Millar has served as a Reviewer for several IEEE publications including IEEE PHOTONICS TECHNOLOGY LETTERS, IEEE JOURNAL OF SELECTED TOPICS IN QUANTUM ELECTRONICS, IEEE COMMUNICATIONS LETTERS, and the IEEE/OSA JOURNAL OF LIGHTWAVE TECHNOLOGY.

Benn C. Thomsen (M'06) received the B.Tech. in optoelectronics, and the M.Sc. and Ph.D. degrees in physics from The University of Auckland, New Zealand. His doctoral research involved the development and characterization of short optical pulse sources suitable for high-capacity optical communication systems.

He then joined the Optoelectronics Research Centre, Southampton University, U.K., as a Research Fellow in 2002, where he carried out research on ultrashort optical pulse generation and characterization, optical packet switching based on optically coded labels, and all-optical pulse processing. He joined the Optical Networks Group, University College London, London, U.K., in 2004, and held an EPSRC Advanced Fellowship from 2006 to 2011 and was appointed as a lecturer in 2007.

Dr. Thomsen's current research focuses on the physical-layer implementation of dynamic optical networks.

Polina Bayvel (S'87–M'89–SM'00–F'10) received the B.Sc. (Eng.) and Ph.D. degrees in electronic and electrical engineering from University College London (UCL), London, U.K., in 1986 and 1990, respectively. Her Ph.D. research focused on nonlinear fiber optics and their applications.

In 1990, she was with the Fiber Optics Laboratory, General Physics Institute, Moscow (Russian Academy of Sciences), under the Royal Society Postdoctoral Exchange Fellowship. She was a Principal Systems Engineer with STC Submarine Systems, Ltd., London, U.K., and Nortel Networks (Harlow, U.K., and Ottawa, ON, Canada), where she was involved in the design and planning of optical fiber transmission networks. During 1994–2004, she held a Royal Society University Research Fellowship at UCL, and, in 2002, she became a Chair in Optical Communications and Networks. She is currently the Head of the Optical Networks Group, UCL. She has authored or co-authored more than 290 refereed journal and conference papers. Her research interests include optical networks, high-speed optical transmission, and the study and mitigation of fiber nonlinearities.

Prof. Bayvel is a Fellow of the Royal Academy of Engineering (F.R.Eng.), the Optical Society of America, the U.K. Institute of Physics, and the Institute of Engineering and Technology. She is a member of the Technical Program Committee (TPC) of a number of conferences, including Proc. ECOC and Co-Chair of the TPC for ECOC 2005. She was the 2002 recipient of the Institute of Physics Paterson Prize and Medal for contributions to research on the fundamental aspects of nonlinear optics and their applications in optical communications systems. In 2007, she was the recipient of the Royal Society Wolfson Research Merit Award.

Seb J. Savory (M'07-SM'11) received the M.Eng., M.A., and Ph.D. degrees in engineering from the University of Cambridge, U.K., in 1996, 1999, and 2001, respectively, and the M.Sc. (Maths) degree in mathematics from the Open University, Milton Keynes, U.K., in 2007.

His interest in optical communications began in 1991, when he joined Standard Telecommunications Laboratories, Harlow, U.K., prior to being sponsored through his undergraduate and postgraduate studies, after which he rejoined Nortel's Harlow Laboratories. In 2005, he joined the Optical Networks Group at University College London (UCL), holding a Leverhulme Trust Early Career Fellowship from 2005 to 2007, and appointed as a University Lecturer in 2007 and subsequently Reader in Optical Fibre Communication in 2012. From Jun. 2009 to Jun. 2010, he was also a Visiting Professor at the Politecnico di Torino, Italy. His current research interests include digital coherent transceivers, optical transmission systems and subsystems, and digital signal processing.

Dr. Savory is Editor-in-Chief of IEEE PHOTONICS TECHNOLOGY LETTERS, Technical Program Chair for OFC 2013, and Technical Program Chair for SPPCom 2012 and SPPCom 2013. In addition, he serves on the Editorial Board for IET Optoelectronics and the technical program committee for the European Conference on Optical Communication and the IEEE Photonics Conference.